Experimental Investigation of Ignition in Turbulent Non-Premixed Bluff-Body Flames

S.F. Ahmed*, T. Marchione†, and E. Mastorakos‡
Engineering Department, University of Cambridge, Cambridge, CB2 1PZ, UK

I. Introduction

Understanding spark-ignition of turbulent flames, especially non-premixed, is not yet at a point that quantitative theoretical predictions can be made, although ignition of non-premixed combustion is important in high-altitude relight of aviation gas turbines, in industrial furnaces, and in some GDI automotive engines. Experiments with spark ignition of jet diffusion flames[1,2] showed that the probability of the emergence of an initial flame kernel in the spark neighbourhood is approximately equal to the probability of finding air-fuel mixture within the flammability limits. This concept has been further explored to provide a quantitative explosion risk assessment[3] with CFD and a presumed shape of the PDF of the mixture fraction. Recently, spark ignition of non-premixed flames has been re-visited with jet[4] and counter-flow[5] flames. It was shown that, if ignition means the achievement of a full diffusion flame and not just the emergence of a small kernel that may be convected with the flow without causing flame ignition, the ignition probability is reduced and can be zero even in locations that have finite probability of flammable mixture fractions. The difference was attributed to local strain effects or high velocities that may not allow the flame kernel to grow or a flame to propagate, despite the local mixture fraction being flammable. In addition, the non-local effects, heat convection from the spark for instance, can play a very important part in determining the success of ignition[5], so that the ignition probability was finite even in regions of zero probability of finding flammable mixtures. Simulations of spark ignition in a laminar non-premixed counterflow flame[6] reproduced these conjectures: ignition of the stoichiometric fluid could be achieved due to heat diffusion from the sparked region, even if that was located at rich or lean positions, and there was a critical strain rate, depending on the spark position and energy, above which ignition could not be achieved.

Our previous experimental work[4,5] has used simplified geometries, so that these fundamental features of ignition of non-premixed combustion could be revealed. This paper presents additional measurements of ignition probability of a new turbulent non-premixed bluff-body burner, which is a geometrical arrangement directly relevant to gas turbine combustors as it involves recirculation and inhomogeneous mixtures. The present data can help with the design of practical ignition systems in realistic combustors and the development of advanced combustion models.

II. Experimental Methods

The burner (Fig.1) consists of two concentric circular ducts of length 400 mm. The inner diameter of the outer duct D_s is 35 mm. The inner duct is a 6 mm internal diameter tube and its end at the burner exit has a conical bluff-body of diameter D_b = 25 mm, giving a blockage ratio $BR = D_b^2/D_s^2 = 50\%$. The flame area was enclosed using a 80 mm long fused silica quartz cylinder of inner diameter 70 mm, which provided optical access for the imaging and also avoided air entrainment from the surrounding. The annulus between the outer and inner ducts serves as the passage for the air, which flows through a 200 mm long plenum of inner diameter 100 mm. The plenum has divergent and convergent cross-sections at the inlet and the exit respectively, which helps to avoid the flow separation during the expansion and contraction. The air flow was streamlined inside the plenum chamber by flow straighteners. The fuel, pure methane, passed through the inner tube all the way along the burner without mixing with the air until it reached the bluff-body. The bluff-body has a certain design to allow the fuel to be injected radially through a 0.7 mm circular gap to the main air flow just 2 mm before the exit of the burner, Fig.1. The aim of this design was to achieve a non-premixed flame with radial fuel injection in order to avoid penetration of the

* PhD student, Engineering Department, University of Cambridge, Cambridge, CB2 1PZ, UK.
† Post-doct, Engineering Department, University of Cambridge, Cambridge, CB2 1PZ, UK.
‡ Reader, Engineering Department, University of Cambridge, CB2 1PZ, UK.Email: em257@eng.cam.ac.uk

recirculation zone and hence increase mixing and flame stability. The air velocity at the exit was mainly at U_a = 10 m/s and, for limited experiments, U_a = 15 m/s. The fuel velocity at the exit area of the bluff-body gap was ranging from U_f = 4 to 8 m/s. Both air and fuel flow rates were controlled by mass flow controllers.

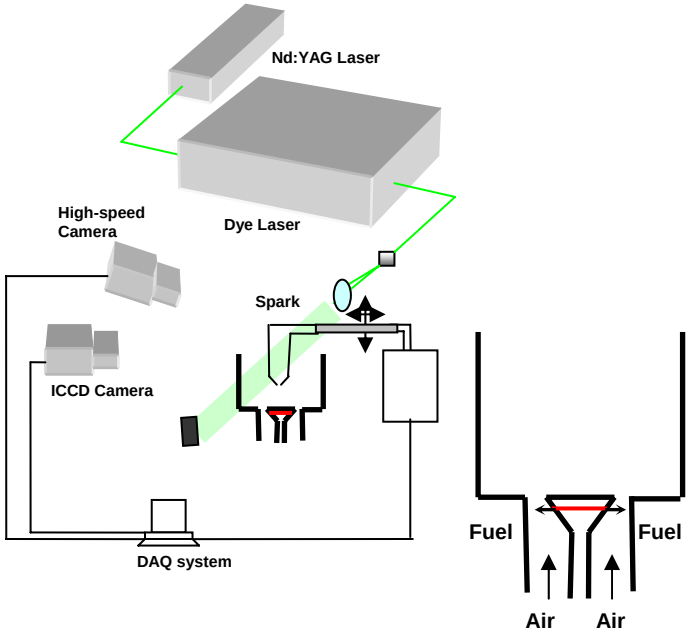

Figure 1. Schematic diagram of the test rig and the optical layout for PLIF imaging.

An ignition system was especially designed to produce repeatable sparks whose energy and duration could be varied independently. The main features of the unit can be found in Ref. 4 and followed the practice of Ref. 7. The spark was created between two tungsten electrodes of 1 mm diameter, which were placed as shown in Fig.1 to ensure minimum disturbance to the flow field. The electrodes had pointed edges to reduce the heat loss from the spark and the distance between them was 2 mm. The two electrodes were attached to a twin-bore ceramic tube, which was traversed axially and radially to cover the whole flow field with 0.1 mm resolution. For the experiments described here, the spark had duration of 500 μs and the electrical energy delivered by the circuit was 200 mJ. For each position, 50 independent spark events were performed and the percentage of events resulting in a flame establishment gave the ignition probability, P_{ign}.

The mixture fraction has been measured by a HFR500 fast FID hydrocarbon concentration detector with a 1 mm diameter sampling probe. The detector had a respond time of about 0.9 ms and a sample gas flow rate of about 0.5 liter/min. The probe was traversed radially with 0.5 mm steps at z = 10 mm above the bluff-body and axially along the burner centerline with a 3 mm step. The mixture fraction profile was measured for four different cases, as shown in Fig.2. Planar Laser-Induced Fluorescence of the OH radical has been used to examine the flame structure at various instants following the initial kernel generation. The output from a Nd:YAG laser was used to pump a Dye laser (Fig.1). The frequency doubled beam was tuned at 283.00 nm to excite the Q1(6) transition of A-X(1-0) band. The beam was spread into a vertical sheet with thickness of about 0.15 mm, by a combination of a 25-mm focal length cylindrical lens and a 500-mm focal length lens. The laser sheet passed through the centreline of the burner. The OH fluorescence from the (0,0) and (1,1) bands near 310 nm was captured by a Nikkor 50 mm lens and an ICCD camera fitted with a combination of Scott glass UG11 and WG305 filters[7].

The ignition event was also monitored with a Phantom V4.2 Digital High Speed Camera fitted with a fast intensifier. A number of movies were captured with 8100 fps for successful and failed ignition events at different locations in the flow field in order to understand the behavior and the structure of the flame front from the moment of the spark until the establishment of the full planar turbulent flame.

III. Results and Discussion

A. Mixing Field

Figure 2 shows time-average mixture fraction profiles across the recirculation zone and along the burner centerline. Previous velocity filed measurements of this burner[8] show that the width and the height of the recirculation zone of are about 1 and 1.5 D_b respectively. It is evident that mixing inside the recirculation zone is just above the rich flammability limit of methane (ξ_{rich} = 0.089) for conditions B (U_f = 5 m/s) and C (U_f = 8 m/s) shown in Fig.2a. However, for conditions A (U_f = 4 m/s) and D (U_a = 15, U_f = 7.5 m/s), the mixture inside the recirculation zone is flammable. These measurements indicate that the fuel-air mixing in this configuration is very sensitive to the change in fuel and air velocities. Furthermore, conditions B and D have the same global equivalence ratio (ϕ = 0.55), but the mixture fraction is different within the recirculation zone. Figure 2b shows an axial mixture fraction profile for case B (main case). It can be observed that the mixture fraction becomes flammable at about z = 15 mm above the bluff-body. More detailed mixture fraction measurements can be found in Ref. 8.

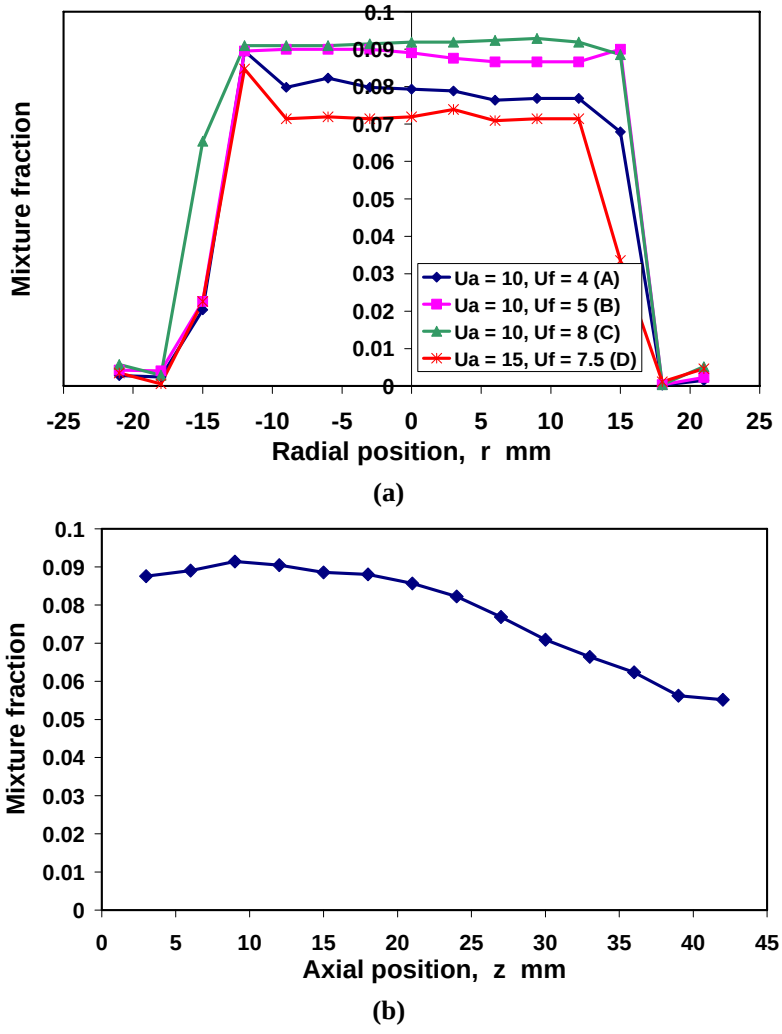

Figure 2. Mean mixture fraction from probe measurements. (a) Radial profile at z = 10 mm; (b) axial profile along the centerline for case (B).

B. Flame Visualization and Structure

The behavior of the flame propagation after the ignition in the bluff-body burner depends more on the ignition location relative to the recirculation zone, rather than on the flow condition. Figure 3 shows high-speed camera

images of a successful ignition event at z = 25 mm, r = 15 mm in the main flow condition used in this work, case B. In this case the flame was ignited outside the recirculation zone, which resulted in axial flame propagation at the beginning to light up that side of the flow first, and then the flame propagated towards the other side in order to establish the flame. It took between 40 to 50 ms, on average, for the flame to stabilize from this ignition location. This flame propagation behavior can be understood as the axial velocity in the location of ignition is much higher than the radial velocity[9] and the mean mixture fraction for this case within the recirculation zone is slightly above $\xi_{rich,}$ Fig. 2a. Therefore, it is expected that the flame propagates in the axial direction first before it propagates radially and tangentially to the other side of the burner. Different propagation behavior can be observed if the ignition happens inside the recirculation zone[8].

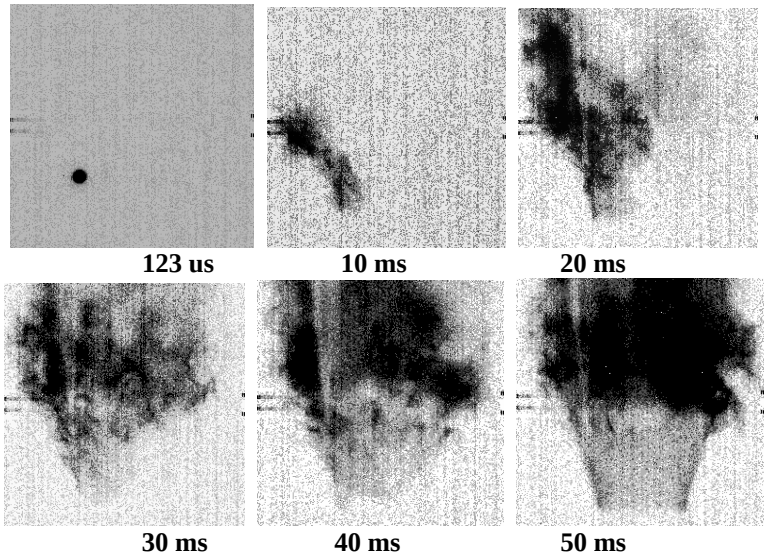

Figure 3. Instantaneous high-speed camera images of an ignition event with 8100 fps and exposure time 113 µs. U_a = 10 m/s, U_f = 5 m/s. Ignition at z = 25 mm, r = 15 mm. The images cover a region of 70×70 mm.

The average OH-PLIF images of about 100 different successful ignition events at different delays from the spark, Fig. 4, show that the flame structure resembles a sphere, which expands toward the bluff-body. However, at certain time, about 12 ms, it starts propagating axially to form the stable flame structure. The OH radical has high concentration around the stoichiometric iso-surface location. It should be noted that, on an instantaneous base, there is no well-defined structure for the flame front (i.e. edge flame of triple flame) during the propagation, contrary to the jet and counterflow geometries[4,5]. In addition, there seems to be a large variability of the flame shape in different ignition events.

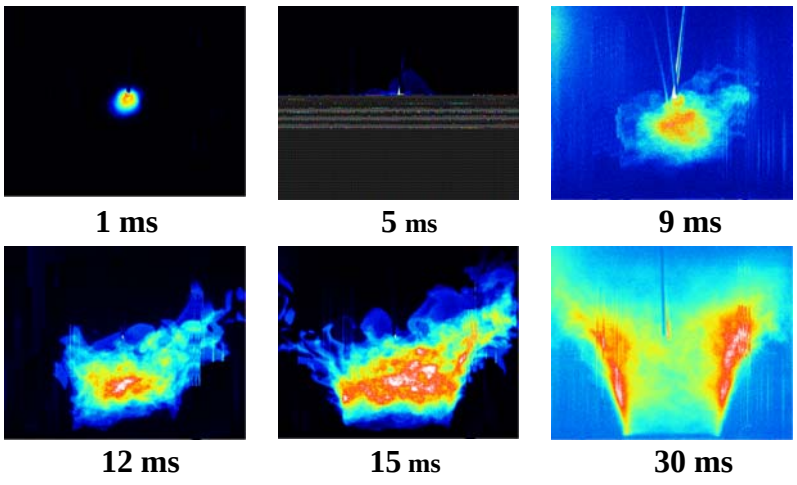

Figure 4. Average OH-PLIF images at different times from the spark. U_a = 10 m/s, U_f = 5 m/s. Ignition at z = 25 mm, r = 0 mm. The images cover a region of 70×50 mm.

C. Ignition Probability

Figure 5 shows the ignition probability contour for the main case B. It can be observed that the highest ignition probability region is located between r = ± 10 to 20 mm and z = 10 to 20 mm, which is located around the stoichiometric mixture fraction (ξ_{st} = 0.055) shown in Fig. 2a. There is some discrepancy between the ignition probability and the mean mixture fraction, since ignition can be achieved in some areas that are above the rich flammability such as the area between z = 0 to 15 mm along the centerline, Fig. 2b. This can be explained partly by the finite mixture fraction fluctuations and partly by the fact that the average axial and radial velocities at this region have high values, 8 m/s and 2.5 m/s respectively[8]. These high velocities can play a role in convecting the heat from the spark location to the flammable region and igniting the flame. A similar observation was found in the counter-flow flame ignition[5]. The other high probability area is between z = 20 and 25 mm at the centerline, which is located within the flammable region. Above z = 30 mm, the flow seems to have a premixed characteristic with global equivalence ratio close to 0.55. That is why the ignition probability above this location becomes uniform with about 10% probability. A more detailed interpretation of this contour needs a measurement of the mixture fraction fluctuation.

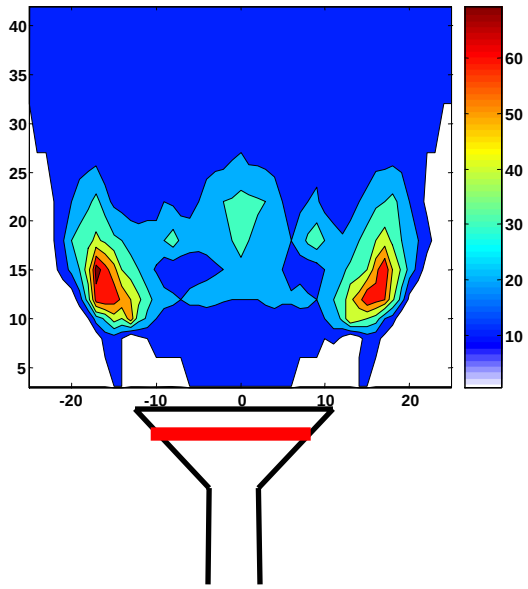

Figure 5. Ignition probability contour of U_a = 10 m/s and U_f = 5 m/s (case B). Spark: 200 mJ and 500 µs.

IV. Conclusion

The success of igniting turbulent non-premixed bluff-body flames of radially injected methane fuel with a spark has been quantified by measuring the ignition probability for various fuel and air velocities. PLIF of OH has also been used to visualize the flame following ignition. The main conclusions from the present work are the following. First, the mixture fraction values show high sensitivity to the fuel and air velocities. In addition, the average flammable region surrounds the recirculation zone. Second, the direct visualization of the ignition events shows that the direction that the flame propagates after the spark depends more on the ignition location than on the flow conditions. Third, instantaneously, the OH-PLIF images show no particular structure of the flame front during propagation due to the strong turbulence. However, on average, the flame expands as a sphere up to certain point when it starts forming the shape of the stable flame. A direct comparison with the ignition probability and the flammability regions will be done in the full paper.

Acknowledgments

This work has been supported by the Department of Trade and Industry and the EPSRC, U.K. and Rolls-Royce plc. We thank Dr. R. Balachandran from UCL for useful discussions and Mr. K. Kalsi of CUED for help with the probe measurements.

References

[1]Birch, A. D., Brown, D. R., and Dodson, M. G., *Proc. Combust. Inst.,* Vol. 18, 1981, pp. 1775-1780.
[2]Birch, A. D., Smith, M. T. E., Brown, D. R., and Fairweather, M., *Proc. Combust. Inst.*, Vol. 21, 1986, pp. 1403-1408.
[3]Alvani, R. F., and Fairweather, M., In *Turbulence, Heat and Mass Transfer*, Vol. 4, 2003, Hanjalic et al. (Eds), pp. 911-918.
[4]Ahmed, S. F., and Mastorakos, E., *Combust. Flame* 146 (2006) 215-231
[5]Ahmed. S. F., Balachandran, R., and Mastorakos, E., *Proc. Combust. Inst.*, Vol. 31, 2007 (To appear).
[6] Richardson, E.S. & Mastorakos, E. Combust. Sci. Tech., Vol. 177, 2007 (To appear).
[7]Balachandran, R., "Experimental investigation of the response of turbulent premixed flames to acoustic oscillation," PhD Dissertation, University of Cambridge, Cambridge, 2005.
[8]Ahmed, S. F., "Spark ignition of turbulent non-premixed flames," PhD Dissertation, University of Cambridge, Cambridge, 2006.